ANTIOXIDANTS & REDOX SIGNALING
Volume 13, Number 9, 2010

DOI: 10.1089/ars.2010.3200

The N-terminal Shuttle Domain of Erv1 Determines the Affinity for Mia40 and Mediates Electron Transfer to the Catalytic Erv1 Core in Yeast Mitochondria

Eirini Lionaki,[1,2] Michalis Aivaliotis,[1] Charalambos Pozidis,[1] and Kostas Tokatlidis[1,3]

Abstract

Erv1 and Mia40 constitute the two important components of the disulfide relay system that mediates oxidative protein folding in the mitochondrial intermembrane space. Mia40 is the import receptor that recognizes the substrates introducing disulfide bonds while it is reduced. A key function of Erv1 is to recycle Mia40 to its active oxidative state. Our aims here were to dissect the domain of Erv1 that mediates the protein–protein interaction with Mia40 and to investigate the interactions between the shuttle domain of Erv1 and its catalytic core and their relevance for the interaction with Mia40. We purified these domains separately as well as cysteine mutants in the shuttle and the active core domains. The noncovalent interaction of Mia40 with Erv1 was measured by isothermal titration calorimetry, whereas their covalent mixed disulfide intermediate was analyzed in reconstitution experiments *in vitro* and *in organello*. We established that the N-terminal shuttle domain of Erv1 is necessary and sufficient for interaction to occur. Furthermore, we provide direct evidence for the intramolecular electron transfer from the shuttle cysteine pair of Erv1 to the core domain. Finally, we reconstituted the system by adding *in trans* the N- and C- terminal domains of Erv1 together with its substrate Mia40. *Antioxid. Redox Signal.* 13, 1327–1339.

Introduction

Most mitochondrial proteins are made in the cytosol and then imported into the organelle by following very versatile and dedicated import pathways (7). The intermembrane space (IMS) of mitochondria has proteins that mediate a variety of vital cellular functions, such as homeostasis of heme and metal ions, transport of metabolites, control of programmed cell death and aging, as well as respiration. Several of the IMS proteins acquire disulfide bonds during their biogenesis, as the key mechanism underpinning their folding (oxidative folding) and retention in the IMS. The substrates of this mitochondrial oxidative-folding pathway are usually proteins of low molecular mass (up to ~20 kDa) (12), do not contain a presequence, and possess cysteines that are organized usually in duplicated CX3C or CX9C motifs. The two most studied examples are the small Tim family, with a twin CX3C motif, and Cox17, with a twin CX9C motif (4, 21, 26). These proteins are substrates for a dedicated machinery that oxidizes them by introducing intramolecular disulfides in a process coupled to their import (9, 20). Unique in this pathway compared with the other mitochondrial import pathways is the fact that neither matrix ATP nor the inner membrane potential is needed; the energy for translocation is instead provided mainly by the covalent modification of the substrate through formation of intramolecular disulfide bonds.

Mia40 and Erv1 constitute the two crucial molecules that operate as a disulfide relay in the oxidative folding pathway in the IMS (5). In the last 5 years, strong evidence that supports a mechanism for coordinated transfer of disulfides has accumulated from studies using mainly *in vitro* reconstituted systems and import in mitochondria. On translocation through the outer membrane (OM) in a reduced and unfolded state, substrates are recognized by Mia40. This step is guided by a recently identified new internal targeting signal found in almost all of the Mia40 pathway substrates. This signal, called MISS (22) or ITS (27), guides the preproteins onto the substrate binding cleft of Mia40 through hydrophobic interactions, thus priming a unique cysteine of the substrate for transient disulfide bond formation ("docking") with the active-site cysteine of Mia40 (27). Through this disulfide exchange reaction, oxidative folding is initiated specifically by Mia40. The relevant pairs of electrons from the substrate that

[1]Institute of Molecular Biology and Biotechnology, Foundation for Research and Technology Hellas (IMBB-FORTH), Crete, Greece.
Departments of [2]Biology and [3]Materials Science and Technology, University of Crete, Heraklion, Crete, Greece.

are transferred initially to Mia40, then pass onto oxidized Erv1, a FAD-dependent sulfhydryl oxidase and from there on to cytochrome *c* and the respiratory chain or cytochrome *c* peroxidase (1, 6, 9). In aerobic conditions, the final electron acceptor is molecular oxygen, but this remains unknown in anaerobic conditions. The role of Erv1 in this process was initially suggested to be the recycling of Mia40 to its oxidized state, based mainly on the accumulation of Mia40 in a reduced state in the absence of Erv1 *in vivo* and the identification of transient disulfides between Erv1 and Mia40 (20). Complementing this evidence, it was demonstrated with purified components that Erv1 can fully oxidize the active-site CPC motif of Mia40 *in vitro* in the absence of any other protein component (3, 16, 30). All this evidence supported the idea that Mia40 is a physiologic protein substrate for Erv1. Although Erv1 does not seem directly to oxidize substrates of the Mia40-Erv1 pathway *in vitro* (1, 30), good evidence suggests that when added in catalytic amounts together with Mia40 in a reconstitution system *in vitro*, this results in complete oxidation of the substrate (30, 32). Furthermore, the isolation of a complex between the substrate, Mia40, and Erv1 has been suggested to imply a direct role of Erv1 in oxidation of the substrate in the context of such a ternary complex *in viv*o (27).

Erv1 belongs to the Erv/ALR sulfhydryl oxidase family that has members in the extracellular environment (Quiescin sulfhydryl oxidase) (18, 19) in poxviruses (E10R) (23, 24) and the endoplasmic reticulum (Erv2) (11, 13, 25, 29). All members of this family bind FAD noncovalently. FAD is used to accept electrons from substrates during oxidation; these are then transferred to oxygen, resulting in generation of hydrogen peroxide (H_2O_2) (31).

The Erv/ALR family members have a catalytic core of ~100 amino acids that stabilizes FAD within a four-helix bundle (33). A conserved redox-active CX2C motif forms the active-site disulfide situated proximal to the isoalloxazine ring of the FAD cofactor. In addition, a flexible tail segment contains another conserved CX2C pair called the "shuttle pair," which can be either at the N-terminus or C-terminus of the protein, with variable spacing from the active-site disulfide for the different Erv/ALR family members (11). Finally, an additional disulfide pair, whose role is to stabilize the FAD cofactor, is not involved in the catalytic reaction (15, 17) ("structural disulfide pair" C159-C176 for yeast Erv1) (Fig. 1). It has been shown in previous studies that the core domain of yeast Erv1 that contains the active-site cysteines (C130–C133) is sufficient to oxidize small substrates like DTT (17). The active-site cysteines receive electrons directly from the substrate, and they transfer them to the nearby FAD moiety. From FAD, the electrons are passed on to downstream electron acceptors. For larger molecules, like TCEP, which is an artificial substrate for Erv1 (3) or Mia40, which is one physiological protein substrate in the mitochondrial intermembrane space, both the shuttle cysteine pair C30-C33 and the active-site cysteine pair C130-C133 are required for electron transfer and oxidation (3, 10, 32). The measured redox potential for each of these cysteine pairs (-320 mV for the shuttle and −150 for the catalytic disulfide pair) is in agreement with a putative intramolecular disulfide bond exchange (9).

In the present study, we investigated the noncovalent interaction between these two protein partners, and we established that the N-terminal shuttle domain of Erv1 is necessary and sufficient for the noncovalent interaction to occur. Based on this observation, and on previous studies, we further followed the first step of Mia40–Erv1 interaction by monitoring the formation of the mixed disulfide intermediate between them *in vitro* and *in organello*. We produced separately the N-terminal shuttle peptide, the ΔN72Erv1 core, and cysteine mutants of either the shuttle cysteine pair (C30/33) or the active-site cysteine pair (C130/133) in full length Erv1, and tested combinations of them for the capacity to form the mixed disulfide intermediate with Mia40. The results suggest that the N-terminal peptide, when oxidized, is necessary and sufficient also for the first disulfide bond with Mia40. Furthermore, we showed for the first time that the core domain of Erv1 can directly oxidize the shuttle cysteine pair of the N-terminal peptide. When the reduced N72 peptide of Erv1 is added *in trans*, with the core domain of the protein and with partially reduced Mia40, the interaction between Mia40 and the N72 shuttle peptide is reconstituted.

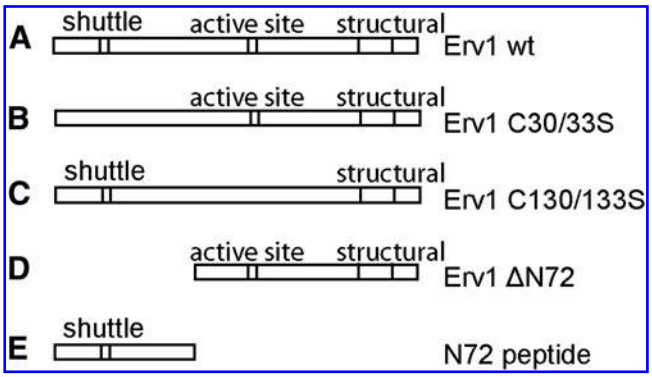

FIG. 1. Schematic representation of the Erv1 variants used in this study. The short vertical lines represent the cysteines of Erv1. From B to E, each variant contains either a functional core domain with the cysteines of the active site intact, or an N-terminal domain with the shuttle cysteine pair intact.

Materials and Methods

Protein expression and purification

The constructs pET24Erv1wt and pET24Erv1ΔN72 were a gift from Dr. Thomas Lisowsky (multiBIND, Biotec, GMBH). The double amino acid substitutions on yeast *ERV1* were generated by PCR-based site-directed mutagenesis (Stratagene QuickChange site-directed mutagenesis kit) by using pET24Erv1wt plasmid as the template. Primer design and the PCR conditions were performed according to the manufacturer's guidelines. The mutations were verified by sequencing reactions. The Erv1 variants (except for the N72 Erv1 peptide) were expressed in BL21 (DE3) rare codon *Escherichia coli* cells. In detail, the cells bearing the expression vector were harvested after induction with 0.1 m*M* IPTG for 16 h at 18°C. The growth of cells was performed in typical Luria Bertani (LB) medium, supplemented with the appropriate antibiotics for selection, and 10 μM FAD. Cells were harvested by centrifugation, resuspended in 300 m*M* NaCl, 50 m*M* Tris HCl, pH 7.4, 10% glycerol, 10 μM FAD, 4 m*M* PMSF, and sonicated. The soluble fraction (which contained the His-tagged protein) was separated by centrifugation (30 min, 21,000 *g*, 4°C), sup-

plemented with 10 m*M* imidazole, and loaded on appropriate amount of preequilibrated Ni-NTA beads (Qiagen). Ni-NTA resin was washed with 50 m*M* NaCl, 50 m*M* Tris HCl, pH 7.4, 10% glycerol, 20 m*M* imidazole, and eluted with 50 m*M* NaCl, 50 m*M* Tris HCl, pH 7.4, 25% glycerol, 200 m*M* imidazole. For the expression of the N72 Erv1 peptide, the nucleotide sequence was PCR amplified with appropriate primers from the wt *ERV1* and cloned in pGEX 4T1 expression vector. The peptide was expressed and purified as previously described for other GST fusion protein (27). Mia40 ΔN290, as well as Mia40 ΔN290 SPS, was expressed from the pET22 expression vector and purified as previously described (27).

Isothermal titration calorimetry

The thermodynamic parameters of Mia40ΔN290SPS binding to Erv1 variants were measured by using a MicroCal VP-ITC microcalorimeter. Experiments were carried out at 25°C, in 50 m*M* phosphate buffer, at pH 7.4. At least two independent measurements of each reaction were performed. Protein concentration in the syringe (Mia40ΔN290SPS) ranged from 0.5 to 0.6 m*M*, whereas protein concentration in the cell (Erv1 variants) ranged from 0.150 to 0.170 m*M*. The heat of dilution of Mia40 was measured by injecting the ligand into the buffer solution.

Construction of the Erv1-depleted strain

A cassette containing the Gal1-10 promoter and the marker gene conferring resistance to geneticin was PCR amplified from M4801 vector with the following primers:

Forward, 5′-GATGCTACAAGTACGTTGTCATCTCAAC CTCTTGATTAAGGGAGCTCGTTTTCGACACTGG-3′

Reverse, 5′-CTTGTGGTGGATTATCCGTCATTTTATCTA TTGCTTTCATGGATCCGTTTTTTCTCCTTGAC-3′

The resulting product was introduced by homologous recombination in the genome of the wt FT5 *Saccharomyces cerevisiae* strain, substituting the endogenous Erv1 promoter. The genetically engineered clones were selected on geneticin plates and then tested by PCR for the insertion of the cassette. For the growth test, the Erv1-depleted strain as well as the wt FT5 parental strain were grown first in YPL (lactate, 2% vol/vol) supplemented with 0.2% galactose, for the first 24 h, and then shifted to the same medium supplemented with 0.2% glucose for another 48 h, before the drop test took place.

Isolation of mitochondria

Wild-type mitochondria and Erv1-depleted mitochondria were isolated from the *Saccharomyces cerevisiae* strain D273-10B and from the Erv1-depleted (FT5 strain), as described previously (4, 14). The yeast strains were grown at 30°C in medium containing 1% (wt/vol) yeast extract, 2% (wt/vol) bacto-peptone, and 2% lactate (vol/vol), pH adjusted to 5.5 (YPL). In the Erv1-depleted strain, the cells were grown in the presence of 0.2% glucose for 24 h before cell harvesting and mitochondrial isolation.

In organello *complementation assay*

For the *in organello* complementation assay, we used isolated Erv1-depleted mitochondria, replenished with several Erv1 variants. For this replenishment, the purified proteins were precipitated by 4-time dilution in saturated ammonium sulfate and incubation for 30 min on ice. The precipitated proteins were pelleted by centrifugation (30 min, 25,000 *g*, 4°C) and resuspended in denaturation buffer (8 *M* urea, 50 m*M* NaCl, 50 m*M* Tris, pH 8.0, 20 m*M* DTT). For complete denaturation, the proteins were incubated at 37°C for 30 min. After denaturation, the precursor proteins were imported in Erv1-depleted mitochondria in the presence of 2 m*M* ATP and 2.5 m*M* NADH for 30 min at 30°C. After this first import reaction, mitochondria were reisolated by centrifugation and resuspended in fresh import buffer for the import reaction of the radioactive precursor, Mia40 SPC. ^{35}S-labeled Mia40 SPC precursor protein was synthesized by using the TNT SP6-coupled transcription/translation kit (Promega), and was subsequently imported in Erv1-depleted yeast mitochondria for the indicated time points at 30°C. The import reaction was blocked by adding 20 m*M* NEM. The unimported material was then digested by incubation of mitochondria with proteinase K (25 μg/ml) for 20 min on ice. PK was inhibited by PMSF (4 m*M*), and mitochondria were reisolated by centrifugation, and were either solubilized in Laemmli sample buffer or in denaturing solibilization buffer for Ni-NTA pull-down assay.

Ni-NTA pull-down assay

After *in organello* complementation assay, mitochondria were resuspended in solubilization buffer (8 *M* urea, 1% Triton X-100, 200 m*M* NaCl, 50 m*M* Tris, pH 8.0, 10 m*M* imidazole, 2 m*M* PMSF) in concentration 1 mg/ml, and incubated at room temperature (RT) for 30 min. The solubilized material was separated from the nonsolubilized by centrifugation at 16,000 *g* for 20 min (RT). After centrifugation, the supernatant was loaded on 25 μl of preequilibrated Ni-NTA beads, and incubated for 1 h (RT), with gentle shaking, for the binding of the His-tagged protein to occur. After binding, the beads were spun down for 30 s at 4,000 *g* (RT), and the unbound material was removed. Beads were washed twice with 500 μl solubilization buffer, and then the bound material was eluted in Laemmli sample buffer and boiled at 95°C. The bound material was separated with SDS-PAGE, and the radioactive Mia40 SPC was visualized with autoradiography.

In vitro *interaction assay*

Mia40ΔN290 was partially reduced (only in the CPC motif) by incubation with 2 m*M* DTT, or 1 m*M* TCEP, for 30 min at 30°C. Then partially reduced Mia40 was 100 times diluted in 50 m*M* NaCl, 50 m*M* Tris, pH 7.4, so that the DTT concentration in the reaction was reduced to 0.2 m*M*. Equimolar amounts of partially reduced Mia40 with Erv1 variants were incubated for the indicated time points at 30°C. The reaction was stopped by adding 20 m*M* NEM, and the samples were separated with nonreducing or reducing SDS-PAGE, and detected by immunodecoration. The removal of DTT from the reduced N72 peptide, before the interaction with partially reduced Mia40ΔN290, was performed by gel filtration with a Sephadex G-25 column.

Thiol-trapping

The N72 Erv1 peptide was either left untreated or reduced with 5 m*M* DTT for 30 min at 30°C (unless otherwise stated) and then incubated with 15 m*M* 4-acetamido-4′-maleimidyl-stilbene-2,2′-disulfonic acid (AMS, Invitrogen), in the presence

of 1% SDS. The samples were incubated for 1.5 h at room temperature and then separated by reducing SDS-PAGE, and detected with immunodecoration.

In gel *trypsin digestion*

The N72 Erv1 peptide was either treated with 5 m*M* DTT for 30 min at 30°C or left untreated, and then incubated for 45 min at room temperature (RT) with 20 m*M* NEM. Subsequently, the samples were loaded on nonreducing SDS-PAGE. The gel was fixed for an hour (RT) in aqueous solution with 30% methanol and 10% acetic acid, and then stained overnight in "Blue Silver" Colloidal Coomassie (0.12% Coomassie G-250, 10% ammonium sulfate, 10% phosphoric acid, and 20% methanol). The gel bands were excised from the gel and cut into small pieces. The gel pieces were destained by successive steps of incubation in 50% acetonitrile in water and 50 m*M* ammonium bicarbonate. After destaining, the gel pieces were incubated with 55 m*M* iodoacetamide for 45 min (RT) and then covered in trypsin solution (4 μg/ml in 50 m*M* ammonium bicarbonate) for 12–16 h at 37°C. After trypsin digestion, the supernatant was collected and pooled together with the solutions from the elution steps that followed (incubation with water, 50% acetonitrile, and 0.1% trifluoroacetic acid (TFA) in 50% acetonitrile). Finally, the eluted tryptic peptides were lyophilized and kept as dry powder at −20°C until further analysis.

N72 Erv1 peptide redox state analysis by mass spectrometry (nLC-ESI-LTQ-Orbitrap ETD)

The dried tryptic peptide mixtures were dissolved in 0.1% formic acid and analyzed on a nano-flow liquid chromatography system (Easy-nLC, Proxeon, Denmark) coupled via a nanoESI source (Proxeon) to an LTQ-Orbitrap XL equipped with an ETD module. Per run, 9 μl of the tryptic peptide mixtures was loaded and on-line desalted on a 100 μm×25 mm C18 trapping column (Easy-Colum, Proxeon; 5 μm) at a flow rate of 0.3 μl/min of buffer A (0.1% formic acid in MiliQ water). By valve switching, the sample was flushed from the trapping-column onto a nanoscale RP-C18 column (75 μm 100 mm, Reprosil-Pur 120, C18-AQ, 3 μm; fused silica emitter column packed in-house), and a binary buffer gradient was started at a constant flow of 0.3 μl/min. Peptides were separated and eluted from the stationary phase by using the following 80-min step-gradient: 5 min in 1% buffer B [0.1% formic acid in acetonitrile (vol/vol), 1–50% buffer B for 55 min, 50–95% buffer B for 5 min, 10 min in 95% buffer B, 95–1% buffer B for 5 min, and equilibration in 1% buffer B for 5 min]. Automated data-dependent acquisition with the mass spectrometer was initiated when the gradient was started. Full-range scans were acquired in Orbitrap (400–1,600 m/z), and the 10 most intense multiply charged ions were automatically selected for optimal fragmentation in LTQ by using collision-induced dissociation (CID) or electron-transfer dissociation (ETD) by using the data-dependent decision tree (DDDT). DDDT automatically selects an optimal fragmentation technique based on peptide properties (charge state, m/z, etc.) for the highest fragmentation efficiencies. The instrument was operated with a spray voltage of 2,300 V, a capillary voltage of 35 V, a tube lens voltage of 140 V, a capillary temperature of 180°C, an AGC MS target value of 10^6, and an Orbitrap resolving power of 60,000 (m/z = 400). Automatic selected precursor ions were subjected either to CID (isolation width 2 Da, normalized collision energy 35%, activation q 0.25, activation time, 30 ms) or ETD (isolation width 2 Da, reaction time 100 ms) and analyzed with the LTQ. Each scan included two microscans, a maximum injection time of 100 ms, and an AGC MS^n target value of 10^4. Dynamic exclusion of fragmented precursors was enabled with the following settings: repeat count, 1; repeat duration, 30 ms; exclusion list size, 500; exclusion duration, 20 ms; and exclusion mass width relative to mass, 10 ppm. Identification of the tryptic peptides of N72 Erv1 peptide was performed by a combination of manual spectra inspection and Proteome Discoverer 1.1 processing, by using both Mascot and Sequest for the database search on Uniprot Yeast database. The following search parameters were used: maximum five missed cleavage sites, cysteine modification by carbamidomethylation and NEM, and methionine oxidation as variable modifications. The tolerance was set as follows: 10 ppm peptide mass tolerance and 0.5 Da MS/MS tolerance.

Miscellaneous

For the separation of proteins <15 kDa, Tris-Tricine SDS–PAGE was applied (2). Quantification of radioactive bands was performed by using the Image Quant software.

Results

Saccharomyces cerevisiae

Erv1 contains six cysteines organized in three pairs that are conserved through evolution (Fig. 1). For this study, we created double cysteine mutants of each of the two redox active cysteine pairs of Erv1, Erv1C30/33S and Erv1C130/133S. These double cysteine mutants together with the wild-type protein, the core domain (ΔN72Erv1), as well as the N-terminal peptide (N72 Erv1 peptide) were expressed in bacteria and purified by affinity chromatography (see Material and Methods). All the Erv1 variants were made as C-terminally His-tagged proteins, except for the N72 peptide, which was expressed as a GST-fusion followed by cleavage from the GST tag with thrombin.

The N-terminus of Erv1 is necessary and sufficient for the noncovalent interaction with Mia40

The C30-C33 cysteine pair of Erv1 has been suggested to interact directly with Mia40 *in vit*ro (3), by analogy to the function of the shuttle disulfide in Erv2 (15), and based on recent evidence for human ALR that was found to interact with human Mia40 only when the long form of ALR (containing the shuttle disulfide) was used (10). However, as no direct evidence on the domain(s) of Erv1/ALR that interacts with Mia40 is available, we wanted to address this question by using yeast Erv1 and monitoring the noncovalent interaction with yeast Mia40. Because the reactive cysteines reside on the N-terminal flexible arm of Erv1, it would make sense to hypothesize that the protein surface responsible for the initial noncovalent interaction between the two proteins resides within this segment. To test this hypothesis, we performed isothermal titration calorimetry (ITC) experiments. It was crucial for this assay to avoid the formation of covalent bonds between the two proteins, as this would mask the protein–protein interaction signal (due to the very high energy of the

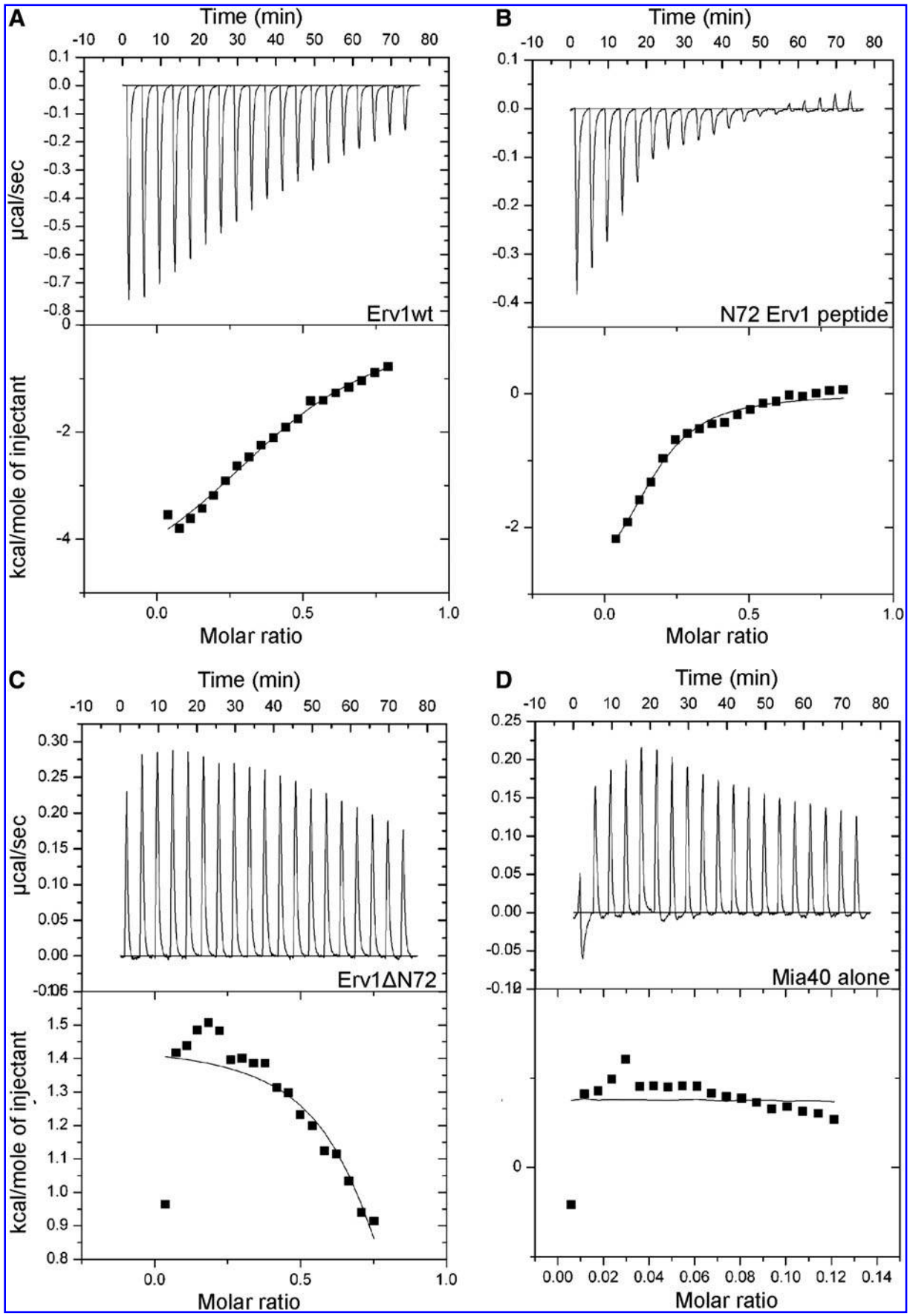

FIG. 2. Thermodynamic analysis of the Mia40-Erv1 interaction. ITC titration curves (*upper panels*) and binding isotherms (*lower panels*) for Mia40ΔN290SPS interaction with (**A**) Erv1wt, (**B**) N72 Erv1 peptide, (**C**) Erv1ΔN72, and (**D**) buffer alone, at 25°C in phosphate buffer (pH 7.4).

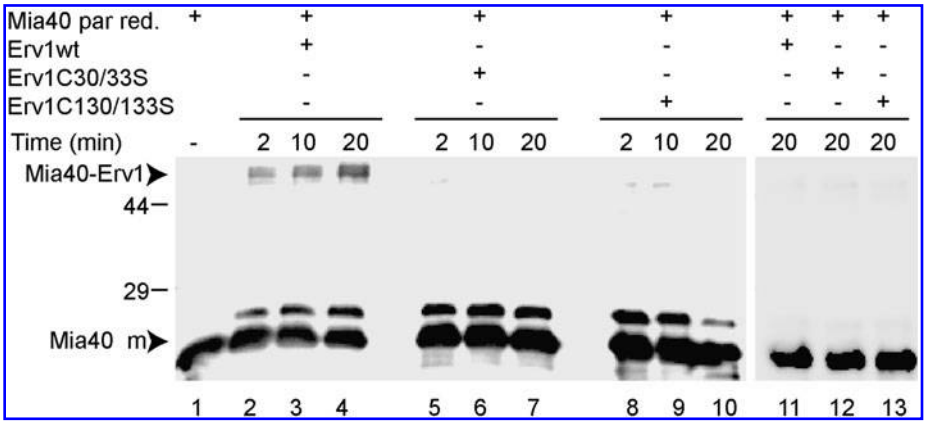

FIG. 3. *In vitro* interaction of partially reduced Mia40ΔN290 with Erv1 variants, to monitor the mixed-disulfide intermediate formation. Mia40ΔN290His, partially reduced, was incubated with Erv1 wt or mutants for the indicated time points. The reaction was blocked by the addition of 20 m*M* NEM, and the samples are loaded either in the absence of reducing agent (*β*Merc) (lanes 1–10), or in the presence of reducing agent (lanes 11–13), for SDS-PAGE. The species of Mia40, Mia40 monomer (Mia40 m), and Mia40-Erv1 mixed-disulfide intermediate (Erv1-Mia40), were detected by immunodecoration with α-Mia40. Molecular-weight markers in kilodaltons are indicated.

covalent bond compared with noncovalent protein interaction). We therefore used as a substrate the ΔN290Mia40SPS version of Mia40 (which includes all the functional core of the wt yeast Mia40 protein), in which both cysteines of the CPC are mutated to serines. This construct was previously used successfully to analyze the protein–protein interactions between Mia40 and the Tim substrates (27). The results are shown in Fig. 2.

The K_d of wt Erv1 interacting with ΔN290Mia40SPS was measured to be 25 μM (Fig. 2A). This value is ~10 times higher than the K_d of interaction of Mia40 with its substrate Tim10 (27 and Discussion). The double C30-C33S mutant of Erv1 has about a 2 times lower but still substantial affinity for Mia40 (data not shown). However, when the N-terminus shuttle segment was removed in the ΔN72Erv1 truncation, binding was essentially abolished (measured at background levels similar to the heat of dilution of Mia40; Fig. 2C and D, respectively). This result suggested that the N-terminus of Erv1 is necessary for the noncovalent interaction with Mia40.

Is it, however, sufficient? To address this, we tested the affinity of the N72 Erv1 peptide alone for ΔN290Mia40SPS. Interestingly, the affinity of the shuttle segment is not only unaffected but even slightly higher than that of the full-length protein (Fig. 2B; the K_d of this interaction was measured at 10 μM). These results show that the N-terminus of Erv1 alone is sufficient for interaction with Mia40.

Both cysteine pairs of Erv1 are important for the formation of a mixed-disulfide intermediate with Mia40 in vitro

To test the ability of each double-cysteine mutant of Erv1 (C30/33S or C130/133S) to form an intermediate with Mia40, we incubated it with partially reduced ΔN290Mia40. Partial reduction of Mia40 (to reduce only the CPC motif) (4, 16) took place by incubating the protein for 30 min with 2 m*M* DTT. The interaction of Erv1 with Mia40 in equimolar amounts was allowed at 30°C for different time points (as indicated; Fig. 3) followed by addition of 20 m*M* NEM. The samples were loaded on nonreducing SDS-PAGE, and the mixed disulfide intermediate (Mia40-Erv1 adduct) was monitored by immunodecoration with anti-Mia40 antiserum. As shown in Fig. 3, the wt Erv1 gives a mixed-disulfide intermediate with Mia40 in a time-dependent manner (lanes 2–4), which is sensitive to reduction by *β*-mercaptoethanol (lane 11). In contrast, the C30/33S double mutant of Erv1 cannot form the first disulfide bond with the partially reduced Mia40 (lanes 5–7), indicating that these two cysteines are involved in the

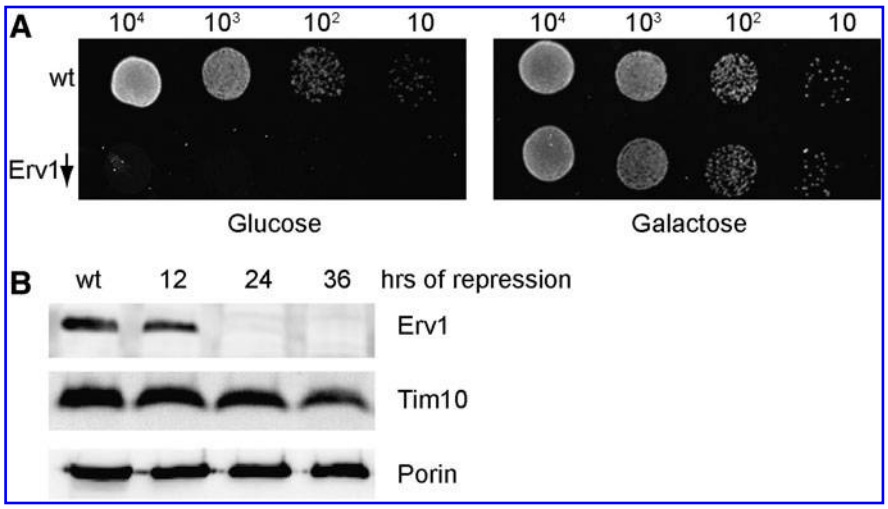

FIG. 4. Construction of an Erv1-depleted strain. (**A**) Growth test of the genetically engineered strain, in which the endogenous ERV1 gene is under the control of the *GAL1-10* inducible promoter (Erv1 ↓), together with the wild-type parental strain (wt), on glucose- or galactose-containing media. (**B**) Isolated mitochondria from wt or Erv1-depleted strain after growth for 12, 24, or 36 h in glucose-containing media, were loaded on SDS-PAGE and then immunoblotted with antibodies for the indicated proteins.

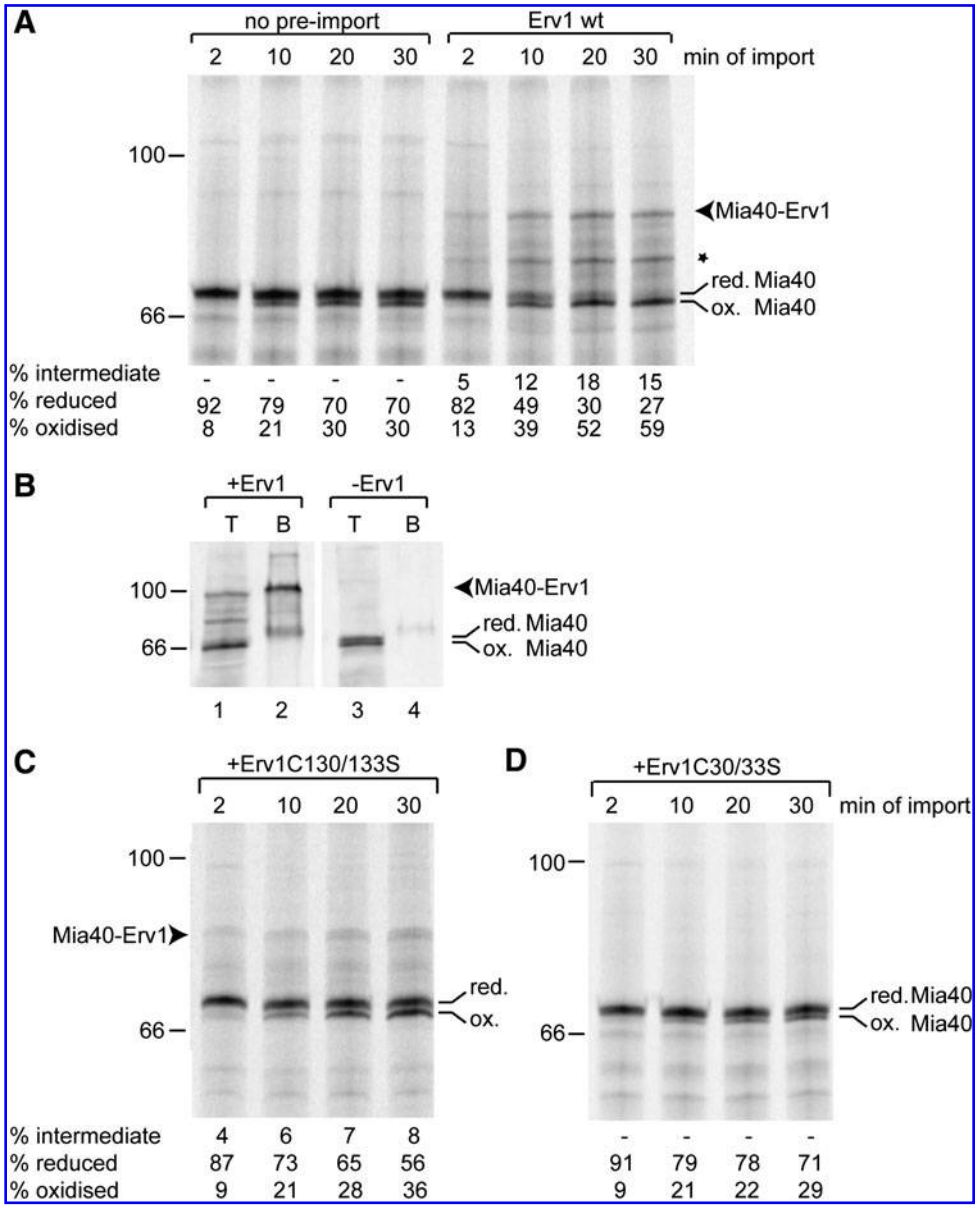

FIG. 5. ***In organello*** **complementation assay to monitor the mixed-disulfide intermediate between the newly incoming radioactive Mia40SPC and the preimported Erv1 variant.** (**A**) Purified Erv1 was denatured and preimported in Erv1-depleted mitochondria for 30 min at 30°C (lanes 5–8). After reisolation of mitochondria and resuspension in import buffer, radioactive Mia40SPC was imported. The import reaction of the radioactive Mia40SPC was stopped at the indicated time points by adding 20 m*M* NEM in the reaction tube. Import of radioactive Mia40 SPC was performed also in mitochondria in which Erv1 was not preimported, for the indicated time points (lanes 1–4). Unimported material was digested with proteinase K (PK). Mitochondria were reisolated by centrifugation and solubilized in nonreducing SDS sample buffer. (**B**) Pull-down assay to verify that the 80-kDa radioactive band is covalently bound to His-tagged Erv1. After preimport of purified wt Erv1 (lanes 1–2) or not (lanes 3–4) in Erv1-depleted mitochondria, import of the radioactive Mia40SPC followed for 30 min at 30°C. After PK treatment, mitochondria were solubilized under denaturing conditions, and then loaded on Ni-NTA beads. In lanes 1 and 3: 50% of the material used for the pull-down assay (T). In lanes 2 and 4, total bound material (B). (**C**) and (**D**), the same as in **A**, but the preimported purified precursors are Erv1C130/133S (**C**) and Erv1C30/33S (**D**). All samples are loaded on nonreducing SDS-PAGE, and autoradiography followed. Molecular-weight markers in kilodaltons are indicated.

formation of this bond *in vitro*. Conversely, the C130/133S mutant of Erv1 has the shuttle cysteine pair intact, but its core domain is mutated. Surprisingly, we see that, although the shuttle cysteine pair is intact in this mutant, it is not enough to attack the reduced CPC motif of Mia40 *in vitro*, when the core of Erv1 (C130-C133) is mutated (lanes 8–10). Identical data were obtained when Mia40 was reduced with TCEP (data not shown).

The formation of mixed-disulfide intermediate in organello *requires the shuttle cysteine pair*

Next, we tried to establish an assay more relevant to the *in vivo* situation, to test our *in vitro* observations. To achieve that, we constructed a yeast strain, in which the endogenous promoter of *ERV1* has been replaced by the *GAL1-10* inducible promoter. This strain is able to grow in the presence of galactose because the *ERV1* gene is expressed, but it stops growing after 48 h in glucose-containing media (Fig. 4A). From this particular strain, we isolated mitochondria after 12, 24, or 36 h of growth in glucose-containing media. Mitochondria were loaded on SDS-PAGE, and the amount of the endogenous proteins was detected with Western blotting (Fig. 4B). The endogenous Erv1 protein is no longer detectable after 24 h of growth in glucose-containing media. As a control, the amount of porin, an outer-membrane protein, is unaffected. Additionally, the amount of Tim10, which is a known substrate for the Mia40-Erv1 pathway, was clearly not so reduced as Erv1, arguing for a specific effect of the Erv1 depletion in short times ($\leq$24 h). For longer times (36 h), the steady-state levels of Tim10 began to be affected. This is in agreement with previous data by which incubation of a *GAL-ERV1* strain in glucose for 48 h showed a marked decrease in the endogenous amounts of small Tims (20).

To reconstitute the system and assay for the ability of each Erv1 mutant to complement the absence of the endogenous protein specifically in the interaction with Mia40, we imported Mia40SPC as a radioactive substrate, in Erv1-depleted mitochondria, after preimport of the different variants of Erv1 purified as His-tagged versions. We chose to use the Mia40SPC variant because it retains the reactive second cysteine of the CPC motif, whereas the mutation of the first cysteine of CPC would help us to monitor better the mixed disulfide intermediate with Erv1 (4, 30). Import of radioactive Mia40SPC in Erv1-depleted mitochondria for the indicated times is shown in Fig. 5A.

After 30 min of import, still ~70% of the precursor remains in the reduced state as it migrates slower on a non-reducing SDS-PAGE. In the second half of panel 5A, we observe that when purified wt Erv1 is preimported in Erv1-depleted mitochondria, at early time points (even 2 min of import of the radioactive Mia40SPC), a new radioactive band appears at ~80 kDa on nonreducing SDS-PAGE (Fig. 5A, lane 5, arrowhead), which disappears in the presence of a reducing agent (data not shown). The intensity of this band increases with time (Fig. 5A, lanes 5–8). This radioactive Mia40-band can be pulled down with Ni-NTA beads, which capture the preimported his-tagged Erv1 protein (Fig. 5B). We therefore conclude that this band represents a Mia40-Erv1 mixed disulfide intermediate between the preimported Erv1 and the radioactive imported Mia40SPC.

A second radioactive band that appears lower than the intermediate band (indicated with an asterisk) does not contain Erv1, as it does not come down on the Ni-NTA pull-down assay in Fig. 5B). The core of the incoming Mia40SPC (defined by the CX9C motifs of Mia40) can be fully oxidized when wt Erv1 is preimported (band indicated as "ox"; Fig. 5A). This oxidation in the presence of preimported wt Erv1 (Fig. 5A, lanes 5–8) proceeds faster than in the absence of Erv1 (Fig. 5A, lanes 1–4), and after 30 min, results in the majority of Mia40 being in the oxidized form (Fig. 5A, lane 8). This reflects the fact that the endogenous Mia40 (which is responsible for the oxidation of the CX9C core disulfides of imported Mia40SPC) (16) can be fully recycled by the preimported Erv1 (imported for 30 min). This, in turn, indicates that in this assay, this part of the Erv1-Mia40 system is reconstituted (Fig. 5A, lanes 5–9).

In conclusion, this assay is helpful in two ways: (a) it allows us to monitor directly the ability of preimported Erv1 to form a mixed-disulfide intermediate with newly imported Mia40SPC, and (b) it allows us to monitor indirectly the recycling of the CPC motif of endogenous Mia40 by monitoring the oxidation state of the Mia40 CX9C core as a substrate of the MIA pathway. The endogenous Mia40 was shown to be oxidized in the twin CX9C core in all cases in mitochondria from the Erv1-depleted strain (Supplemental Fig. 1; *see* www.liebertonline.com/ars). Therefore, the differences we observe in the oxidation of the radioactive substrate should reflect differences in the redox state of the CPC motif of endogenous Mia40, which is modulated by the preimport of the Erv1 variants.

In this assay, we then used the two double-cysteine mutants of Erv1. When the purified Erv1 C130/133S mutant is preimported (Fig. 5C), the radioactive Mia40 precursor forms an 80-kDa species, which is less intense than in the case of preimported wt Erv1. When the C30/33S mutant was preimported (Fig. 5D), the 80-kDa intermediate band was essentially abolished. This result mirrors *in organello* the data obtained *in vitro* (Fig. 3) and supports the concept that the shuttle cysteine pair of Erv1 is absolutely required for the interaction with Mia40, during Mia40 reoxidation. These results demonstrated that, also *in organello,* the existence of a functional active-site cysteine pair is important for the interaction with the newly imported Mia40. As a control, the amounts of the different preimported Erv1 versions in Erv1-depleted mitochondria were confirmed to be comparable by immunostaining with anti-Erv1 antiserum (Supplemental Fig. 1B). Finally, the import of Mia40 was in all cases membrane potential dependent, as expected (Supplemental Fig. 2; *see* www.liebertonline.com/ars). In all cases a full-length version of Mia40 (carrying its presequence) was used for imports. In these assays, the Mia40 presequence is not cleaved, and the protein is hence retained in the inner membrane (data not shown) (8).

The N-terminal shuttle domain of full-length Erv1 can act in trans *to restore the formation of a mixed-disulfide intermediate with Mia40 in mitochondria*

The result that the C30/33S mutant is completely inactive in making the mixed disulfide with Mia40, but the C130/133S instead still maintains some capacity to form this intermediate, led us to test the possibility that the N-terminal shuttle may function *in trans* with the core of Erv1, even when these are present on different molecules. To address this possibility, we performed import experiments in which a mixture of Erv1 versions was preimported. We preimported (a) a mixture of C130/133S together with the C30/33S (Fig. 6A, lanes 5–8) or (b) C130/133S with ΔN72 (Fig. 6A, lanes 9–12). In the first case, a functional core domain comes from the C30/33S mutant and a functional shuttle from the C130/133S mutant, whereas in the second case, a functional core domain comes from the ΔN72 mutant and the functional shuttle from the C130/133S mutant (the functional domains are indicated schematically with grey shades, whereas the inactive, cysteine-mutated domains are shown with an X). We basically observed that, in both cases, we had a substantial restoration of the capacity of the C130/133S mutant to form the intermediate with newly imported Mia40 (arrowhead). Quantification of the intermediate with Mia40 shows restoration to comparable levels with the intermediate formed by preimported wt Erv1 (Fig. 6A, lanes 1–4). Using the mutant C130/133S alone in several independent experiments resulted in ~50% the level of the Mia40-intermediate obtained with the wt Erv1 (data not shown). As an additional control, Ni-NTA pull-down assays (using as input twice the amount corresponding to the 30-min time point of Fig. 6A) confirmed the interaction with Mia40 (Fig. 6B).

Taken together, these data suggest that a functional shuttle N-terminal domain is vital for the formation of the crucial mixed-disulfide intermediate of Erv1 with Mia40 and that this may function even *in trans*, in intermolecular combination with another Erv1 molecule.

In vitro *reconstitution of the Mia40-Erv1 interaction mediated by the N72 Erv1 shuttle domain of full-length Erv1*

Is the Mia40 intermediate formation, mediated by interactions *in trans* between the shuttle and the core of Erv1 *in organello,* an intrinsic capacity of Erv1 that can also be observed

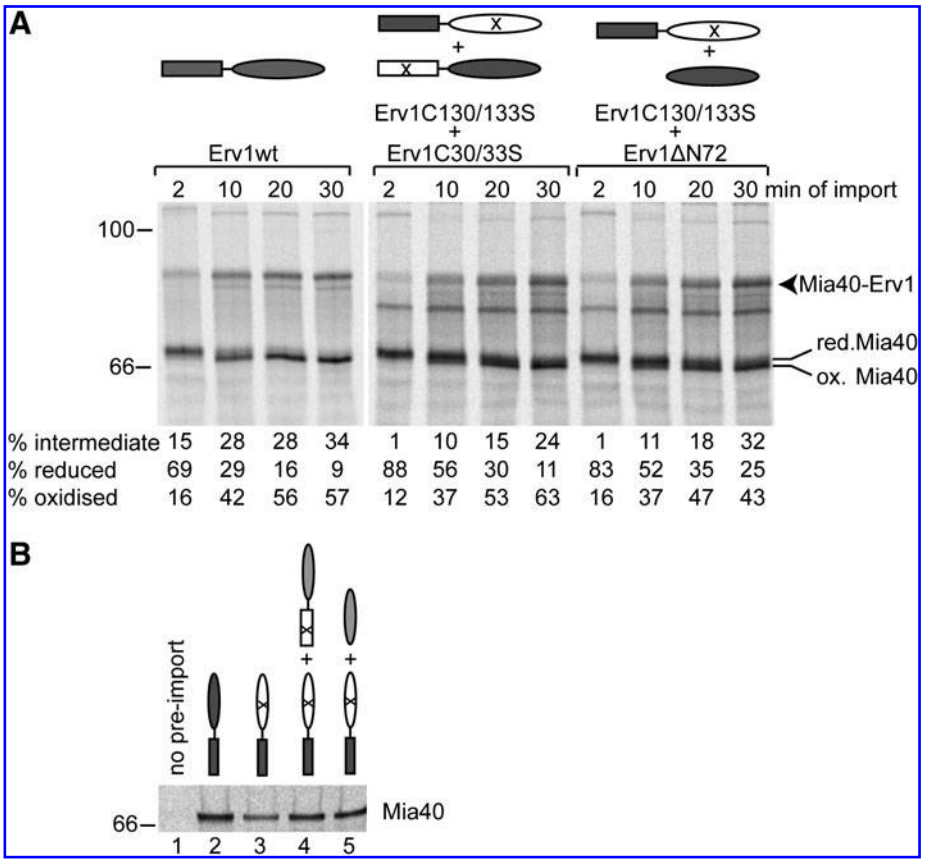

FIG. 6. Intermolecular Erv1 interaction complements the Mia40-intermediate formation and the oxidation of newly incoming Mia40SPC. (**A**) *In organello* complementation assay, where the pre-imported precursors are mixtures of either Erv1C130/133S and Erv1C30/33S (lanes 5–8) or Erv1C130/133S and Erv1ΔN72 (lanes 9–12). Samples are loaded on nonreducing SDS-PAGE, and autoradiography followed. (**B**) Pull-down assay after import of radioactive Mia40SPC for 30 min at 30°C in Erv1-depleted mitochondria supplemented with the indicated Erv1 variants. Pre-imported precursors: lane 1, none; lane 2, Erv1 wt; lane 3, Erv1C130/133S; lane 4, mixture of Erv1C130/133S and C30/33S; lane 5, mixture of Erv1C130/133S with Erv1ΔN72. The bound material from each pull-down assay was separated by reducing SDS-PAGE, and autoradiography followed. Molecular-weight markers in kilodaltons are indicated.

in vitro? To address this point, we performed an *in vitro* experiment similar to the one shown in Fig. 3 but using a combination of C130/133S with C30/33S (Fig. 7, lane 3) or C130/133S with ΔN72 (Fig. 7, lane 4). In both cases, a clear increase in the intermediate with Mia40 is seen compared with C130/133S alone (lane 2). As before (Fig. 3, lanes 2–4), and in agreement with previous *in vitro* reconstitution results (16), wt Erv1 can efficiently interact with partially reduced Mia40 (Fig. 7, lane 5).

It is therefore clear that also *in vitro*, the two domains of Erv1 can cooperate intermolecularly, so that an efficient intermediate with Mia40 is formed.

The N72 Erv1 peptide added in trans *with a functional core Erv1 can restore interaction with Mia40*

These data of Figs. 6 and 7, in combination with the capacity of the N72 domain to retain the full thermodynamic affinity for Mia40, suggested that the N72 added *in trans* should be sufficient to assure interaction with Mia40. We tested this possibility directly in the *in vitro* binding assay (Fig. 8). The N72 peptide was overexpressed and purified as a GST-fusion cleaved off the GST tag and oxidized by air oxidation. Its oxidized state (with an intramolecular disulfide bond between the two cysteines 30 and 33 of the shuttle) was confirmed in two independent ways: (a) by AMS-thiol trapping assay, and (b) by an MS-based analysis (Fig. 9).

To determine the redox state of the peptide N72 of Erv1, the peptide was treated with NEM to block free (reduced) cysteine residues, purified by a nonreducing SDS-PAGE, and after in-gel tryptic digestion of the isolated Coomassie-stained peptide band, it was analyzed on an nLC-ESI-LTQ-Orbitrap. As a

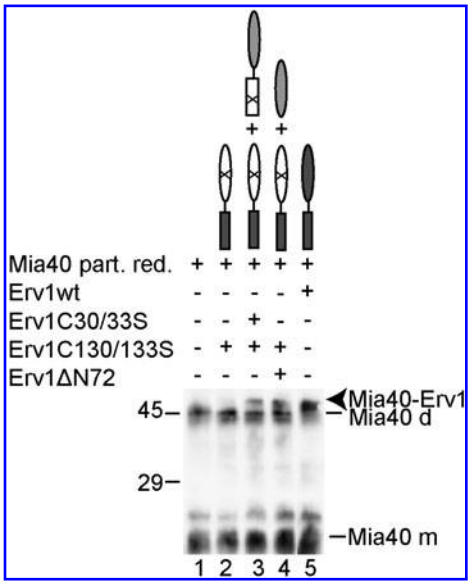

FIG. 7. Intermolecular communication is an intrinsic capacity of Erv1 protein. *In vitro* interaction of partially reduced Mia40ΔN290 with Erv1 wt (lane 5), Erv1C130/133S (lane 2), and mixtures of either Erv1C130/133S with Erv1C30/33S (lane 3) or Erv1C130/133S with Erv1ΔN72 (lane 4). The samples are loaded on nonreducing SDS-PAGE, and the Mia40 species are detected by immunodecoration. Molecular-weight markers in kilodaltons are indicated.

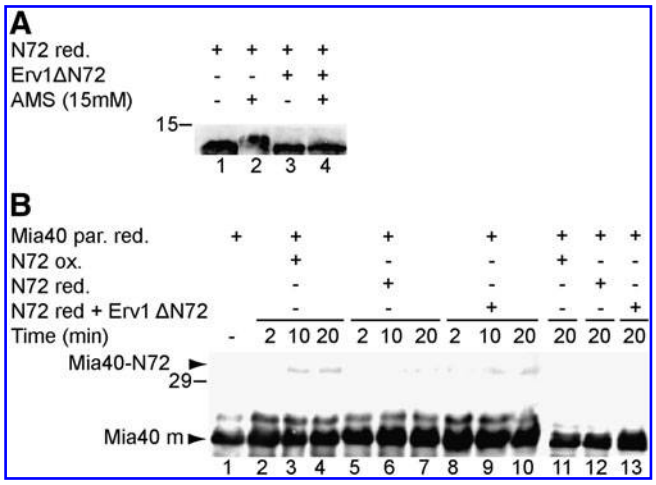

FIG. 8. The N72 shuttle peptide added *in trans* ensures mixed-disulfide intermediate formation with Mia40. (**A**) Reduced N72 Erv1 peptide is reoxidized by incubation with Erv1ΔN72 for 30 min at 30°C. The redox state of the peptide after overnight reduction with 10 mM DTT, which was then removed by gel filtration, before (lanes 1 and 2) and after incubation with Erv1 core (lanes 3 and 4), was monitored by AMS thiol-trapping assay. (**B**) *In vitro* interaction of partially reduced Mia40ΔN290 (alone in lane 1) with oxidized N72 Erv1 peptide (lanes 2–4), reduced N72 Erv1 peptide (lanes 5–7), or reduced and then reoxidized N72 peptide, by incubation with Erv1ΔN72 (lanes 8–10). The reaction between Mia40 and N72 peptide was stopped at the indicated time points, by addition of NEM. Samples in lanes 1–10 are loaded without reducing agent, whereas samples in lanes 11–13 are loaded with *β*Merc on SDS-PAGE and immunodecorated with anti-Mia40 antiserum. Molecular-weight markers in kilodaltons are indicated.

control, the peptide was reduced with DTT and treated with NEM before an identical analysis. Database search and manual inspection of the LC-MS/MS data yielded a reliable identification by tandem mass spectrometry with both CID and ETD (Fig. 9C and D, respectively) of a tryptic peptide of N72 corresponding to the oxidized peptide KIIYDEDGKPCRSC NTLLDFQYVTGK (amino acid sequence 20–45, monoisotopic mass 3003.476 Da) (Fig. 9). This oxidized tryptic peptide of N72 contains a disulfide bond between the residues C30 and C33 and a tryptic missed cleavage on residue R31, probably due to steric hindrance of the disulfide bond. As shown in Fig. 9A, this oxidized peptide is present only in the N72 sample and not in the N72 sample reduced by DTT, indicating that the N72 Erv1 peptide is oxidized *in vitro*. In addition, mass spectrometry data showed that the reduction of N72 Erv1 peptide with DTT before the analysis led to the full reduction of C30–C33 disulfide bond and the subsequent tryptic proteolysis on R31 (Fig. 9A, Supplemental Fig. 3; *see* www.liebertonline.com/ars). In this analysis, two tryptic peptides KIIYDEDGKPCR (amino acid sequence 20–31, monoisotopic mass 1,560.78 Da) and SCNTLLDFQYVTGK (amino acid sequence 32–45, monoisotopic mass 1,312.828 Da) with their C residues reduced and modified by NEM were identified in the reduced-by-DTT N72 Erv1 peptide (Supplemental Fig. 3). These two peptides were not present in the non-reduced-by DTT N72 Erv1 peptide, providing strong evidence that N72 Erv1 peptide is fully oxidized *in vitro*.

AMS thiol-trapping of the peptide confirmed the MS-analysis results. The N72 peptide was either left untreated (Fig. 9B, lanes 1–2) or reduced with 5 m*M* DTT (Fig. 9B, lanes 3–4) and incubated with AMS (Fig. 9B, lanes 2, 4). Reducing SDS-PAGE and immunodecoration with anti-Erv1 antiserum were used to reveal the Erv1 peptide band.

When the N72 peptide with the shuttle cysteine pair oxidized was presented to partially reduced Mia40 (incubated with 1 m*M* TCEP, for 30 min at 30°C to reduce only the CPC motif), the formation of the intermolecular species between N72 and Mia40 was observed (Fig. 8B, lanes 2–4). By contrast, when the reduced form of the N72 peptide was added, the intermediate was essentially abolished (Fig. 8B, lanes 5–7). This result shows that the N72 peptide when oxidized is necessary and sufficient for the formation of the disulfide bond between the shuttle cysteine pair and the CPC motif of Mia40.

Furthermore, we wanted to identify the exact role of the core domain of Erv1 in this interaction, because our previous data show that when this is mutated, the formation of the Erv1-Mia40 intermediate is affected both *in vitro* (Figs. 3 and 7) and *in organello* (Figs. 5 and 6). One logical assumption would be to assume that the core domain of Erv1 is important for the oxidation of the N-terminal shuttle cysteine pair, which in turn oxidizes the CPC of Mia40. To test this, we incubated the N72 peptide after full reduction (incubated with 10 m*M* DTT and passed through gel filtration to remove DTT; see Materials and Methods) with equimolar amounts of the functional core ΔN72Erv1. The redox state of the N72 peptide was then analyzed by AMS thiol-trapping and found to be clearly oxidized (Fig. 8A). This shows that the core Erv1 can indeed oxidize the N72 peptide shuttle cysteine pair. Moreover, when the N72 peptide in a reduced state is incubated with partially reduced Mia40, in the presence of the core ΔN72Erv1, the formation of the intermolecular intermediate between N72 and Mia40 is now restored (Fig. 8B, lanes 8–10). These data reflect the transfer of electrons between the N and C domains of Erv1 *in trans* (from the N to the C domain), which is vital for the function of the Erv1 oxidase on its substrate Mia40.

Discussion

The interaction between Mia40 and Erv1 is at the core of the disulfide relay that underpins oxidative folding of proteins targeted to the mitochondrial IMS. Strong evidence *in vivo* and *in vitro* suggests that the sulfhydryl oxidase Erv1 interacts with Mia40, reduced in its active-site CPC motif, to recycle it to its functional oxidized state. However, the detailed mechanism of action of Erv1 remains unknown. Recent work by Thorpe and colleagues (10) showed that electron transfer between reduced human Mia40 and ALR, the human homologue of Erv1, can only occur *in vitro* with full-length ALR that retains its N-terminal shuttle domain. Additionally, Ang and Lu (3) showed that for the yeast Mia40 and Erv1, an intermolecular electron transfer between the shuttle and the core disulfides of Erv1 is necessary for full oxidation to occur *in vitro*. These studies point to the idea that the shuttle disulfide of Erv1/ALR recognizes substrates first and then interacts intra- or intermolecularly with the core disulfide, following an electron-transfer reaction similar to that occurring for the Erv1 homologue Erv2 that resides in the ER (15). However, no direct evidence for the *in vivo* role of the shuttle disulfide pair of Erv1 is yet available, and the molecular interactions between the two Erv1 domains (shuttle and core) are yet to be understood.

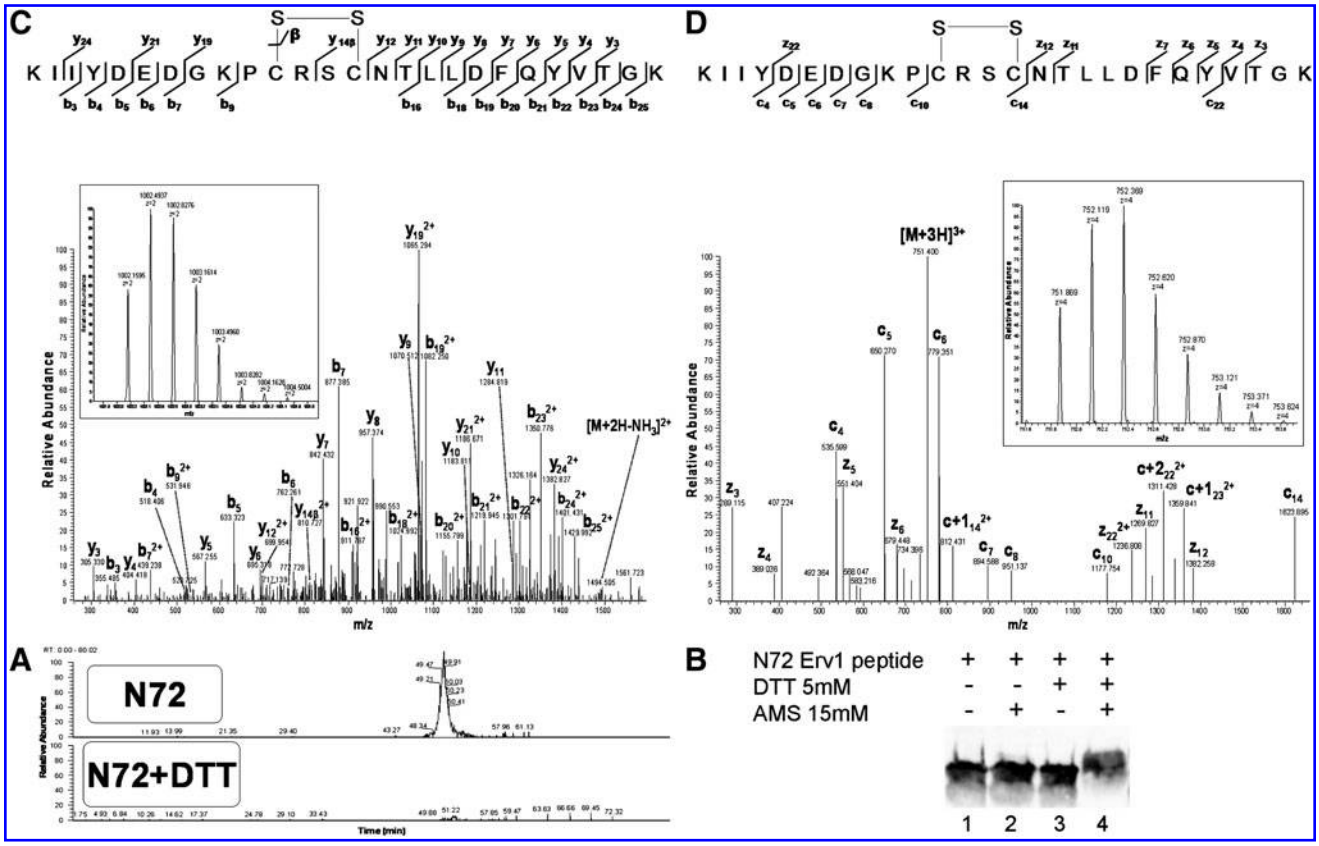

FIG. 9. Determination of the redox state of N72 Erv1 peptide by using in parallel nano-flow liquid chromatography coupled online with a LTQ-Orbitrap tandem mass spectrometer and AMS thiol-trapping. (**A**) A tryptic peptide of N72 Erv1 peptide corresponding to the oxidized peptide KIIYDEDGKPCRSCNTLLDFQYVTGK (amino acid sequence 20–45; monoisotopic mass, 3003.476 Da) was identified in the nonreduced with DTT peptide (upper panel) by using nano-flow liquid chromatography coupled online with an LTQ-Orbitrap tandem mass spectrometer after in-gel tryptic digestion. As it is shown in the extracted ion chromatograms of those untreated (upper panel) and treated (lower panel) with DTT N72, this tryptic peptide disappears after reduction of the N72 Erv1 peptide with DTT, which is due to the reduction of the disulfide bond and its subsequent proteolytic cleavage on Arg31. These findings indicate that the N72 Erv1 peptide is mostly oxidized *in vitro*. (**B**) AMS thiol-trapping assay: The N72 peptide used in this study untreated (lanes 1 and 2) or reduced with 5 mM DTT (lanes 3 and 4) is incubated with AMS (lanes 2 and 4). Samples were separated on reducing SDS-PAGE and detected by immunodecoration (**C**, **D**). Product ion spectra of the +2 (1,002.195 m/z) and +4 (751.869 m/z) charged oxidized tryptic peptide KIIYDEDGKPCRSCNTLLDFQYVTGK of N72 by tandem mass spectrometry (MS/MS) by using two different fragmentation techniques CID (**C**) and ETD (**D**), respectively, as described in Materials and Methods. These MS/MS spectra confirm the presence of a disulfide bond between the residues C30 and C33.

Here we analyzed the thermodynamic interactions between Mia40 on the one hand and each of the two domains of Erv1 on the other, in a first approach to dissect the important protein–protein interactions between Erv1 and its first physiological protein substrate Mia40. We found that the N-terminal shuttle is necessary and sufficient for the protein–protein interaction with Mia40 to occur, which provides solid support for the idea that the shuttle of Erv1 confers specificity for the interaction with Mia40 (10). However, the fact that this interaction is characterized by a physiologically relevant but relatively low thermodynamic affinity (K_d 25 μM) indicates that Erv1 does not have such a stringent specificity for Mia40 and leaves open the possibility that the interaction with Mia40 is very transient and that Erv1 may have additional physiological protein substrates. The predicted structural flexibility of the shuttle domain would support its putative capacity to bind many different substrates, but with low affinity. In this respect, it is interesting that the core of Erv1, devoid of its shuttle, retains substantial sulfhydryl oxidase activity against small substrates, as shown both for the yeast (17) and the human (10) enzyme. One could then rationalize the function of Erv1 as a combination of two important factors: a very potent oxidase whose enzymatic activity is retained by the core, and a structurally maleable shuttle domain that could interact with different substrates with low stringency.

It is therefore important to identify other putative protein substrates for Erv1. In terms of the oxidative folding pathway, the fact that the affinity of Erv1 for Mia40 is about one order of magnitude lower than the affinity of Mia40 for its substrate (27) indicates that the latter is the one that commits the substrate specifically to this pathway.

The N-terminal domain of Erv1 is necessary and sufficient for the interaction with Mia40 to occur when this N-terminal shuttle domain is oxidized. In the cell, the role of the C-terminal core of Erv1 seems to be to oxidize directly its N-terminal shuttle domain so that the latter can now in turn oxidize Mia40. The two domains can even act *in trans* to assure electron transfer from Mia40 to the N-terminal shuttle domain

of Erv1 and from then on to its C-terminal FAD-containing core. Our *in vitro* and *in organello* results support that intermolecular communication between the shuttle domain and the catalytic core of Erv1 is essential for the oxidation of Mia40. These findings provide a mechanistic framework for a more detailed understanding of the molecular interactions underpinning the oxidative folding process in mitochondria.

Acknowledgments

This work was supported by funds from IMBB-FORTH, the University of Crete, and the European Social Fund and national resources (to K.T.). Mass-spectrometry analysis was performed in the Proteomics Facility of IMBB-FORTH that was set up through an FP7-EU–RegPot grant. We thank members of our laboratory for helpful discussions and comments, Thomas Lisowsky for plasmids, and Lily Karamanou for help with ITC.

Author Disclosure Statement

The authors declare no competing financial interests.

References

1. Allen S, Balabanidou V, Sideris DP, Lisowsky T, and Tokatlidis K. Erv1 mediates the Mia40-dependent protein import pathway and provides a functional link to the respiratory chain by shuttling electrons to cytochrome c. *J Mol Biol* 353: 937–944, 2005.
2. Allen S, Lu H, Thornton D, and Tokatlidis K. Juxtaposition of the two distal CX3C motifs via intrachain disulfide bonding is essential for the folding of Tim10. *J Biol Chem* 278: 38505–38513, 2003.
3. Ang SK and Lu H. Deciphering structural and functional roles of individual disulfide bonds of the mitochondrial sulfhydryl oxidase Erv1p. *J Biol Chem* 284: 28754–28761, 2009.
4. Banci L, Bertini I, Cefaro C, Ciofi-Baffoni S, Gallo A, Martinelli M, Sideris DP, Katrakili N, and Tokatlidis K. MIA40 is an oxidoreductase catalyzing oxidative protein folding in mitochondria, *Nat Struct Mol Biol* 16: 198–206, 2009.
5. Bihlmaier K, Mesecke N, Kloeppel C, and Herrmann JM. The disulfide relay of the intermembrane space of mitochondria: an oxygen-sensing system? *Ann N Y Acad Sci* 1147: 293–302, 2008.
6. Bihlmaier K, Mesecke N, Terziyska N, Bien M, Hell K, and Herrmann JM. The disulfide relay system of mitochondria is connected to the respiratory chain. *J Cell Biol* 179: 389–395, 2007.
7. Chacinska A, Koehler CM, Milenkovic D, Lithgow T, and Pfanner N. Importing mitochondrial proteins: machineries and mechanisms. *Cell* 138: 628–644, 2009.
8. Chacinska A, Pfannschmidt S, Wiedemann N, Kozjak V, Sanjuan Szklarz LK, Schulze-Specking A, Truscott KN, Guiard B, Meisinger C, and Pfanner N. Essential role of Mia40 in import and assembly of mitochondrial intermembrane space proteins. *EMBO J* 23: 3735–3746, 2004.
9. Dabir DV, Leverich EP, Kim SK, Tsai FD, Hirasawa M, Knaff DB, and Koehler CM. A role for cytochrome c and cytochrome c peroxidase in electron shuttling from Erv1. *EMBO J* 26: 4801–4811, 2007.
10. Daithankar VN, Farrell SR, and Thorpe C. Augmenter of liver regeneration: substrate specificity of a flavin-dependent oxidoreductase from the mitochondrial intermembrane space. *Biochemistry* 48: 4828–4837, 2009.
11. Fass D. The Erv family of sulfhydryl oxidases. *Biochim Biophys Acta* 1783: 557–566, 2008.
12. Gabriel K, Milenkovic D, Chacinska A, Muller J, Guiard B, Pfanner N, and Meisinger C. Novel mitochondrial intermembrane space proteins as substrates of the MIA import pathway. *J Mol Biol* 365: 612–620, 2007.
13. Gerber BO, Meng EC, Dotsch V, Baranski TJ, and Bourne HR. An activation switch in the ligand binding pocket of the C5a receptor. *J Biol Chem* 276: 3394–3400, 2001.
14. Glick BS. Protein import into isolated yeast mitochondria. *Methods Cell Biol* 34: 389–399, 1991.
15. Gross E, Sevier CS, Vala A, Kaiser CA, and Fass D. A new FAD-binding fold and intersubunit disulfide shuttle in the thiol oxidase Erv2p. *Nat Struct Biol* 9: 61–67, 2002.
16. Grumbt B, Stroobant V, Terziyska N, Israel L, and Hell K. Functional characterization of Mia40p, the central component of the disulfide relay system of the mitochondrial intermembrane space. *J Biol Chem* 282: 37461–37470, 2007.
17. Hofhaus G, Lee JE, Tews I, Rosenberg B, and Lisowsky T. The N-terminal cysteine pair of yeast sulfhydryl oxidase Erv1p is essential for in vivo activity and interacts with the primary redox centre. *Eur J Biochem* 270: 1528–1535, 2003.
18. Hoober KL, Glynn NM, Burnside J, Coppock DL, and Thorpe C. Homology between egg white sulfhydryl oxidase and quiescin Q6 defines a new class of flavin-linked sulfhydryl oxidases. *J Biol Chem* 274: 31759–31762, 1999.
19. Hoober KL, Joneja B, White HB 3rd, and Thorpe C. A sulfhydryl oxidase from chicken egg white. *J Biol Chem* 271: 30510–30516, 1996.
20. Mesecke N, Terziyska N, Kozany C, Baumann F, Neupert W, Hell K, and Herrmann JM. A disulfide relay system in the intermembrane space of mitochondria that mediates protein import. *Cell* 121: 1059–1069, 2005.
21. Milenkovic D, Gabriel K, Guiard B, Schulze-Specking A, Pfanner N, and Chacinska A. Biogenesis of the essential Tim9-Tim10 chaperone complex of mitochondria: site-specific recognition of cysteine residues by the intermembrane space receptor Mia40. *J Biol Chem* 282: 22472–22480, 2007.
22. Milenkovic D, Ramming T, Muller JM, Wenz LS, Gebert N, Schulze-Specking A, Stojanovski D, Rospert S, and Chacinska A. Identification of the signal directing Tim9 and Tim10 into the intermembrane space of mitochondria. *Mol Biol Cell* 20: 2530–2539, 2009.
23. Senkevich TG, White CL, Koonin EV, and Moss B. A viral member of the ERV1/ALR protein family participates in a cytoplasmic pathway of disulfide bond formation. *Proc Natl Acad Sci U S A* 97: 12068–12073, 2000.
24. Senkevich TG, White CL, Koonin EV, and Moss B. Complete pathway for protein disulfide bond formation encoded by poxviruses. *Proc Natl Acad Sci U S A* 99: 6667–6672, 2002.
25. Sevier CS, Cuozzo JW, Vala A, Aslund F, and Kaiser CA. A flavoprotein oxidase defines a new endoplasmic reticulum pathway for biosynthetic disulphide bond formation. *Nat Cell Biol* 3: 874–882, 2001.
26. Sideris DP and Tokatlidis K. Oxidative folding of small Tims is mediated by site-specific docking onto Mia40 in the mitochondrial intermembrane space. *Mol Microbiol* 65: 1360–1373, 2007.
27. Sideris DP, Petrakis N, Katrakili N, Mikropoulou D, Gallo A, Ciofi-Baffoni S, Banci L, Bertini I, and Tokatlidis K. A novel intermembrane space targeting signal primes cysteines for docking onto Mia40 in mitochondrial oxidative folding. *J Cell Biol* 187: 1007–1022, 2009.
28. Stein G, and Lisowsky T. Functional comparison of the yeast scERV1 and scERV2 genes. *Yeast* 14: 171–180, 1998.

29. Stojanovski D, Milenkovic D, Müller JM, Gabriel K, Schulze-Specking A, Baker MJ, Ryan MT, Guiard B, Pfanner N, and Chacinska A. Mitochondrial protein import: precursor oxidation in a ternary complex with disulfide carrier and sulfhydryl oxidase *J Cell Biol* 183: 195–202, 2008.
30. Terziyska N, Grumbt B, Kozany C, and Hell K. Structural and functional roles of the conserved cysteine residues of the redox-regulated import receptor Mia40 in the intermembrane space of mitochondria. *J Biol Chem* 284: 1353–1363, 2009.
31. Thorpe C and Coppock DL. Generating disulfides in multicellular organisms: emerging roles for a new flavoprotein family. *J Biol Chem* 282: 13929–13933, 2007.
32. Tienson HL, Dabir DV, Neal SE, Loo R, Hasson SA, Boontheung P, Kim SK, Loo JA, and Koehler CM. Reconstitution of the mia40-erv1 oxidative folding pathway for the small tim proteins. *Mol Biol Cell* 20: 3481–3490, 2009.
33. Wu CK, Dailey TA, Dailey HA, Wang BC, and Rose JP. The crystal structure of augmenter of liver regeneration: a mammalian FAD-dependent sulfhydryl oxidase. *Protein Sci* 12: 1109–1118, 2003.

Address correspondence to:
Kostas Tokatlidis
Institute of Molecular Biology and Biotechnology
Foundation for Research and Technology Hellas (IMBB-FORTH)
Heraklion 71110
Crete
Greece

E-mail: tokatlid@imbb.forth.gr

Date of first submission to ARS Central, March 22, 2010; date of acceptance, April 1, 2010.

Abbreviations Used

ALR = augmenter of liner regeneration
AMS = 4-acetamido-4′-maleimidylstilbene-2, 2′-disulfonic acid
CID = collision-induced dissociation
CPC = cystein-proline-cysteine
DDDT = data-dependent decision tree
DTT = Dithiothreitol
ERV1 = essential for respiration and vegetative growth
ESI = electrospray ionization
ETD = electron-transfer dissociation
IMS = intermembrane space
ITC = isothermal titration calorimetry
ITS = intermembrane space–targeting signal
LTQ = linear trap quadrupole
MISS = mitochondrial import and sorting signal
NEM = *N*-ethyl maleimide
nLC = nano liquid chromatography
PCR = polymerase chain reaction
RP = reverse phase
RT = room temperature
SDS-PAGE = sodium dodecyl sulfate–polyacrylamide gel electrophoresis
TFA = trifluoroacetic acid

This article has been cited by:

1. Afroditi Chatzi , Kostas Tokatlidis . The Mitochondrial Intermembrane Space: A Hub for Oxidative Folding Linked to Protein Biogenesis. *Antioxidants & Redox Signaling*, ahead of print. [Abstract] [Full Text HTML] [Full Text PDF] [Full Text PDF with Links]
2. Lucia Banci, Ivano Bertini, Simone Ciofi-Baffoni, Deepa Jaiswal, Sara Neri, Riccardo Peruzzini, Julia Winkelmann. 2012. Structural characterization of CHCHD5 and CHCHD7: Two atypical human twin CX9C proteins. *Journal of Structural Biology* . [CrossRef]
3. Emmanouela Kallergi, Maria Andreadaki, Paraskevi Kritsiligkou, Nitsa Katrakili, Charalambos Pozidis, Kostas Tokatlidis, Lucia Banci, Ivano Bertini, Chiara Cefaro, Simone Ciofi-Baffoni, Karolina Gajda, Riccardo Peruzzini. 2012. Targeting and Maturation of Erv1/ALR in the Mitochondrial Intermembrane Space. *ACS Chemical Biology* 120201095624007. [CrossRef]
4. Lucia Banci, Ivano Bertini, Vito Calderone, Chiara Cefaro, Simone Ciofi-Baffoni, Angelo Gallo, Kostas Tokatlidis. 2012. An Electron-Transfer Path through an Extended Disulfide Relay System: The Case of the Redox Protein ALR. *Journal of the American Chemical Society* 120106074929003. [CrossRef]
5. Rajesh Ghai, Robert J. Falconer, Brett M. Collins. 2012. Applications of isothermal titration calorimetry in pure and applied research-survey of the literature from 2010. *Journal of Molecular Recognition* **25**:1, 32-52. [CrossRef]
6. L. Banci, I. Bertini, V. Calderone, C. Cefaro, S. Ciofi-Baffoni, A. Gallo, E. Kallergi, E. Lionaki, C. Pozidis, K. Tokatlidis. 2011. Molecular recognition and substrate mimicry drive the electron-transfer process between MIA40 and ALR. *Proceedings of the National Academy of Sciences* **108**:12, 4811-4816. [CrossRef]
7. Johannes M. Herrmann , Jan Riemer . 2010. Oxidation and Reduction of Cysteines in the Intermembrane Space of Mitochondria: Multiple Facets of Redox Control. *Antioxidants & Redox Signaling* **13**:9, 1323-1326. [Abstract] [Full Text HTML] [Full Text PDF] [Full Text PDF with Links]